NON-SPECULAR REFLECTION OF BOUNDED BEAMS FROM MULTILAYER FLUID-IMMERSED ELASTIC STRUCTURES: COMPLEX RAY METHOD REVISITED

Smaine Zeroug and Leopold B. Felsen

Department of Electrical Engineering / Weber Research Institute
Polytechnic University
Farmingdale, N.Y. 11735

INTRODUCTION

The excitation of various types of leaky waves in layered elastic media by beams incident from an exterior fluid at or near the leaky wave phase-matching angle is of interest for NDE applications. In particular, much attention has been given to the non-specular reflection of beams under such conditions of incidence. While various methods have been employed to study and clarify these phenomena for well collimated beams in plane layered environments [1-11], much less has been done on the corresponding effects when the incident beams are diverging and/or when the layers are curved. To extend the plane layer results to more general conditions, it is desirable to employ analytic modeling that adapts the wave phenomenology locally from planar to curved geometries. Because the phenomena occur in the range of high frequencies, ray field modeling affords an attractive option. By the complex-source-point (CSP) technique, which places a radiating source at a complex coordinate location, a conventional line or point source excited field can be converted into a two- or three-dimensional quasi-Gaussian beam field that is an exact solution of the dynamical equations [12,13]. When the CSP field interacts with a plane or cylindrically layered elastic medium, the resulting internal and external fields can be expressed rigorously in terms of wavenumber spectral integrals [14]. Asymptotic reduction of these integrals, achieved by the method of saddle points applied to deformed contours in the complex spectral wavenumber plane, accounts for all relevant wave phenomena. For the reflected field, this yields explicit waveforms which are synthesized by interacting specularly reflected beam, leaky wave, and possible lateral wave contributions.

The solution strategy outlined above has been applied here to arbitrarily collimated beams that impinge on plane and cylindrically layered geometries at or near the phase matching condition for a leaky wave. For the plane layered environment, the arbitrarily collimated beam formulas developed in this paper for the reflected field at all observation angles and distances reduce near phase matched incidence, and for the well-collimated and paraxial regime, to the non-specular results in the literature [1]. It is also shown that diverging beams incident at the phase-

Review of Progress in Quantitative Nondestructive Evaluation, Vol. 11
Edited by D.O. Thompson and D.E. Chimenti, Plenum Press, New York, 1992

matching angle give rise to a more complex reflected pattern than do well-collimated beams, owing to the more extended and nonuniform interaction region between the specularly reflected and the leaky wave field, which is established by the diverging beam. For the same reason (extended nonuniform interaction region) this behavior is obtained as well for the case of well-collimated beams incident upon a cylindrical interface. The entire formulation is two-dimensional. The three-dimensional case is in preparation.

The paper is organized as follows. The analytical foundation for plane and cylindrically layered elastic structures is presented in Sec.I, with incorporation of the CSP method and the asymptotic reductions. The asymptotic constituents include incident, specularly reflected, and leaky wave fields that are generated by a CSP-extended line source. The specular and leaky wave parts are treated by uniform asymptotics to account for their strong interaction near the phase-matching condition. Numerical results for beams with various collimations impinging on planar and cylindrical water-aluminum interfaces are shown and interpreted in Sec.II. Final remarks about the advantages of the complex ray method conclude the presentation.

FORMULATION

We consider two-dimensional scattering of the pressure field $\mathcal{P}$ excited by a line source in a fluid in the presence of a submerged plane or cylindrically layered elastic structure. With the source located at $\underline{\rho}'$, the time-harmonic pressure field $\mathcal{P}$ at an observation point $\underline{\rho}$ in the fluid can be derived from a displacement potential field Φ,

$$\mathcal{P}(\underline{\rho},\underline{\rho}') = -\rho_f \, \omega^2 \, \Phi(\underline{\rho},\underline{\rho}') \tag{1}$$

where ρ_f is the fluid density, ω is the source frequency and a time dependence $\exp\{-i\omega t\}$ is suppressed. The potential field in the fluid satisfies the source-excited Helmholtz equation with boundary conditions that account for the layered elastic structure, in addition to a radiation condition at infinity. Solution of these boundary value problems is effected in the spectral wavenumber domain corresponding to the space coordinate tangential to the layer boundaries [13]. For the plane layered $\underline{\rho}=(x,y)$ geometry, with the layer interfaces along x, the spectral wavenumber is denoted by k, whereas for the cylindrically layered $\underline{\rho}=(\rho,\phi)$ geometry, with the layer interfaces along ϕ, the spectral wavenumber is ν. With a caret denoting spectral domain quantities, the spectral decomposition yields for the planar and cylindrical cases, respectively,

$$\Phi_{pl}(x,y;x',y') = \frac{1}{2\pi}\int_{-\infty}^{+\infty} \hat{\Phi}_{pl}(k;y,y') \exp\{ik(x-x')\}\, dk \tag{2a}$$

$$\Phi_{cyl}(\rho,\rho';\phi,\phi') = \frac{1}{2\pi}\int_{-\infty}^{+\infty} \hat{\Phi}_{cyl}(\nu;\rho,\rho') \exp\{i\nu(\phi-\phi')\}\, d\nu \tag{2b}$$

Note that k has the dimensions of length^{-1} while ν is dimensionless. In (2b), the physical $-\pi \le \phi \le \pi$ azimuthal domain has been extended to $-\infty < \phi < \infty$ in order to remove the 2π-periodicity constraint from the azimuthal wave spectra. This extension, which allows the inclusion of angularly traveling waves with arbitrary angular periodicity, properly describes high frequency phenomena arising from localized

interactions as in the present study [15]. The reduced forms of the wave equations for the planar and cylindrical cases are solved to yield [16]

$$\hat{\Phi}_{pl}(k;y,y') = \frac{i}{2\kappa_f}\left[\exp\{i\kappa_f|y-y'|\} + R(k)\exp\{i\kappa_f|y+y'|\}\right], \tag{3}$$

$$\kappa_f = \sqrt{k_f^2 - k^2}\ , \quad \begin{cases} \mathrm{Re}\{\kappa_f\} > 0 \text{ if } |k| < k_f \\ \mathrm{Im}\{\kappa_f\} > 0 \text{ if } |k| > k_f \end{cases} \tag{3a}$$

$$\hat{\Phi}_{cyl}(\nu;\rho,\rho') = \frac{i\pi}{4}\left\{H_\nu^{(2)}(k_f\rho_<) + R(\nu)\frac{H_\nu^{(2)}(k_f a)}{H_\nu^{(1)}(k_f a)}H_\nu^{(1)}(k_f\rho_<)\right\}H_\nu^{(1)}(k_f\rho_>);\ \rho,\rho' > a \tag{4}$$

where $k_f = \omega/v_f$ and v_f is the sound speed in the fluid, while $R(k)$ and $R(\nu)$ are, respectively, the spectral domain reflection coefficients accounting for the scattering environment [16].

Equations (2), (3), and (4) represent the formal solutions for line-source-excited inputs. The total field excited by a beam input can be constructed via the complex-source-point (CSP) technique [12]. With a tilde $\tilde{}$ denoting a complex coordinate as well as functions of a complex coordinate, the line source is displaced into the complex coordinate plane via

$$x' \to \tilde{x}' = x' + ib\sin\alpha_o, \quad y' \to \tilde{y}' = y' + ib\cos\alpha_o, \quad b\,real > 0, \quad -\pi \le \alpha_o \le +\pi \tag{5a}$$

$$\rho' \to \tilde{\rho}' = \sqrt{\tilde{x}'^2 + \tilde{y}'^2}\,, \mathrm{Re}\{\tilde{\rho}'\} \ge 0; \quad \phi' \to \tilde{\phi}' = \tan^{-1}\left\{\tilde{x}'/\tilde{y}'\right\} \text{ with } \tilde{\phi}' = \pi \text{ when } \tilde{x}' = 0 \tag{5b}$$

The real-space field radiated by this complex source is a beam with quasi-Gaussian amplitude profile whose maximum lies along the angular direction α_o. The 1/e beam width w_o at the waist (x',y') is given by $w_o = (2b/k_f)^{1/2}$, which establishes b as the Fresnel length of the beam. Note that substitution of the complex extensions (5) into (2), (3) and (4) yields exact formal solutions for the beam input.

The exact spectral integrals representing Φ in the fluid can be evaluated asymptotically by the saddle point method applied in the complex wavenumber plane. Typically, one deforms the integration contour from the real axis in the complex k or ν plane, along which the integrand is highly oscillatory, into the steepest descent path (SDP) passing through the stationary (saddle) point of the phase of the integrand. The dominant contribution to the high frequency field then arises from the saddle point and from the singularities (poles and branch points) intercepted during the SDP deformation. Non-specular reflection of bounded beams, which is the concern of this study, is characterized by the strong interaction of the reflected beam field contributed by the saddle point and a leaky wave pole singularity of the spectral reflection coefficient. This strong interaction, generated by phase matching between the incident beam and the leaky wave, manifests itself by the close proximity of the leaky wave pole and the saddle point, thereby requiring uniform asymptotics in the

reduction of the spectral integrals [14]. For the planar case, the final expression for the total potential field in the fluid is found to be given by

$$\tilde{\Phi}_{\rm pl}(\rho,\rho') \sim \frac{\exp\{i\pi/4\}}{2\sqrt{2\pi}} \frac{\exp\{ik_f \tilde{l}_i\}}{\sqrt{k_f \tilde{l}_i}} + \tilde{R}(\tilde{k}_s) \frac{\exp\{i\pi/4\}}{2\sqrt{2\pi}} \frac{\exp\{ik_f(\tilde{l}'+\tilde{l})\}}{\sqrt{k_f(\tilde{l}'+\tilde{l})}}$$

$$-\frac{1}{4} \frac{\mathrm{Res}\{R(\tilde{k})\}_{k_p}}{(k_f^2 - k_p^2)^{1/2}} \mathit{erfc}(-i\tilde{s}_b) \exp\{i\tilde{P}^{\rm r}_{\rm pl}(k_p)\} + \frac{i}{4\pi} \frac{\mathrm{Res}\{R(\tilde{k})\}_{k_p}}{(k_f^2 - k_p^2)^{1/2}} \frac{\sqrt{\pi}}{\tilde{s}_b} \exp\{i\tilde{P}^{\rm r}_{\rm pl}(\tilde{k}_s)\} \quad (6)$$

where

$$\tilde{P}^{\rm r}_{\rm pl}(\tilde{k}) = [\tilde{k}(x-\tilde{x}') - \sqrt{k_f^2 - \tilde{k}^2}(z+\tilde{z}')] \quad (6a)$$

$$\tilde{l}' = -\tilde{y}'/\cos\tilde{\theta}_s \ , \tilde{l} = -y/\cos\tilde{\theta}_s \ , \tilde{\theta}_s = \tan^{-1}\left[-\frac{x-\tilde{x}'}{y+\tilde{y}'}\right] \quad (6b)$$

For the cylindrical case,

$$\tilde{\Phi}_{\rm cyl}(\rho,\rho') \sim \frac{\exp\{ik_f \tilde{l}_i + i\pi/4\}}{2\sqrt{2\pi k_f \tilde{l}_i}} + \tilde{R}(\tilde{\nu}_s) \frac{\exp\{ik_f(\tilde{l}'+\tilde{l}) + i\pi/4\}}{2\sqrt{2\pi k_f(\tilde{l}'+\tilde{l})}} \sqrt{\frac{a(\tilde{l}'+\tilde{l})\sin\tilde{\gamma}_a}{2\tilde{l}'\tilde{l} + a(\tilde{l}'+\tilde{l})\sin\tilde{\gamma}_a}\Big|_{\tilde{\nu}_s}}$$

$$-\frac{1}{4k_f} \frac{\mathrm{Res}\{R(\tilde{\nu})\}_{\nu_p}}{(\rho\tilde{\rho}'\sin\tilde{\gamma}\sin\tilde{\gamma}'\big|_{\nu_p})^{1/2}} \mathit{erfc}(-i\tilde{s}_b) \exp\{i\tilde{P}^{\rm r}_{\rm cyl}(\nu_p)\}$$

$$+\frac{i}{4\pi} \frac{\mathrm{Res}\{R(\tilde{\nu})\}_{\nu_p}}{k_f(\rho\tilde{\rho}'\sin\tilde{\gamma}\sin\tilde{\gamma}'\big|_{\nu_p})^{1/2}} \frac{\sqrt{\pi}}{\tilde{s}_b} \exp\{i\tilde{P}^{\rm r}_{\rm cyl}(\tilde{\nu}_s)\} \quad (7)$$

where

$$\tilde{P}^{\rm r}_{\rm cyl}(\tilde{\nu}) = k_f(\rho\sin\tilde{\gamma} + \tilde{\rho}'\sin\tilde{\gamma}' - 2a\sin\tilde{\gamma}_a) - \tilde{\nu}(\tilde{\gamma} + \tilde{\gamma}' - 2\tilde{\gamma}_a - [\phi - \tilde{\phi}']) \quad (7a)$$

$$\tilde{l}' = \tilde{\rho}'\sin\tilde{\gamma}' - a\sin\tilde{\gamma}_a\big|_{\tilde{\nu}_s} \ , \quad \tilde{l} = \rho\sin\tilde{\gamma} - a\sin\tilde{\gamma}_a\big|_{\tilde{\nu}_s} \quad (7b)$$

$$\tilde{\gamma} = \cos^{-1}\left(\tilde{\nu}/k_f\rho\right), \qquad \tilde{\gamma}' = \cos^{-1}\left(\tilde{\nu}/k_f\tilde{\rho}'\right), \qquad \tilde{\gamma}_a = \cos^{-1}\left(\tilde{\nu}/k_f a\right) \quad (7c)$$

In the above,

$$\tilde{s}_b = \sqrt{i\left[\tilde{P}^{\rm r}_{\rm pl,cyl}(\zeta_s) - \tilde{P}^{\rm r}_{\rm pl,cyl}(\zeta_p)\right]}, \quad \zeta \equiv k \text{ (planar) or } \nu \text{ (cylindrical)} \quad (8a)$$

$$\mathit{erfc}(z) = \frac{2}{\sqrt{\pi}} \int_z^\infty \exp\{-q^2\}\, dq \quad (8b)$$

$$\tilde{l}_i = \sqrt{(x-\tilde{x}')^2+(y-\tilde{y}')^2}\,, \qquad \mathrm{Re}\{\tilde{l}_i\} \geq 0 \tag{8c}$$

The spectral variables $\tilde{k}_s$ and $\tilde{\nu}_s$ denote the complex saddle point value, while k_p and ν_p denote the pole singularity of the reflection coefficient R which is approximated by

$$\tilde{R}(\varsigma) = \frac{\varsigma-\varsigma_o}{\varsigma-\varsigma_p}\,, \quad \varsigma_o = \varsigma_p^* \tag{9}$$

with the asterisk expressing the complex conjugate. The commonly used simple form of (9) (see [1]) accounts for the relevant spectral phenomena associated with nonspecular reflection, in particular, the main splitting due to the close proximity of a pole and a zero in (9). The first two terms in (6) or (7) represent, respectively, the incident or direct beam field and the specularly reflected beam field. The third term accounts primarly for the leaky wave field in isolation and partly (via the complementary error function *erfc*(z)) for the strong (leaky wave)-(reflected beam) interaction, while the fourth term accounts for the strong interaction effects not included in the third term. When the observer moves outside the strongly interacting nonspecular reflection region, the third term reduces to the isolated leaky wave field plus a remainder, which is now canceled by the fourth term. The breakup into the third and fourth terms as shown is convenient for numerical computation over the entire regime near, or far from, the nonspecular region.

NUMERICAL RESULTS

The numerical results presented below implement (6) and (7) for a water-aluminum interface under conditions where the incident Gaussian beam is nearly or exactly phase matched to the leaky Rayleigh wave. Accordingly, for the planar case, the leaky wave spectral pole is located at [1],

$$k_p = k_p^{\,r} + i\,k_p^{\,i}\,; \qquad k_p^{\,r} = k_f \sin(30.593^o), \quad k_p^{\,i} = 0.01494\,k_f \tag{10}$$

For the cylindrical case, assuming locally planar conditions, the corresponding spectral pole is obtained via the relation [16]

$$k = \nu/a \tag{11}$$

which for a cylindrical interface of radius $a=40$ yields

$$\nu_p = \nu_p^{\,r} + i\,\nu_p^{\,i}\,; \qquad \nu_p^{\,r} = 127.9, \quad \nu_p^{\,i} = 3.75 \tag{11b}$$

The CSP-source is located at

$$(x',y') = (0,-20)\text{--planar geometry;}\quad (x',y') = (10,-50)\text{--cylindrical geometry} \tag{12}$$

In the above, and henceforth, all distances are normalized to the fluid wavelength. Figures 1 to 3 contain typical samples of results extracted from a comprehensive data set that will be presented in greater detail elsewhere [16]. Figure 1 depicts schematically three beam-interface combinations, together with the wave periodicities induced along the interface over the extent of the incident beam. The

mechanism that establishes these periodicities is discussed in the caption of Fig.1. For the well collimated beams in Figs.1(a) and 1(c), the interfaces are well inside the Fresnel region, whereas for the strongly diverging beam in Fig.1(b), the interface is well outside the Fresnel region. When the various induced periodicities, which generate the geometrically reflected beam, interact with the constant periodicity of the leaky wave, the outcome are different interference effects, which lead to splitting of the composite reflected field. For case (a), interference nulls are far apart , whereas for cases (b) and (c), the reflected beam and leaky wave constituents are in and out of phase repeatedly over the interaction region, thereby producing patterns with multiple minima and maxima (multiple splitting). These qualitative predictions are confirmed in Figs.2 and 3. The conventionally observed splitting due to the reflection coefficient zero in (9) occurs in addition.

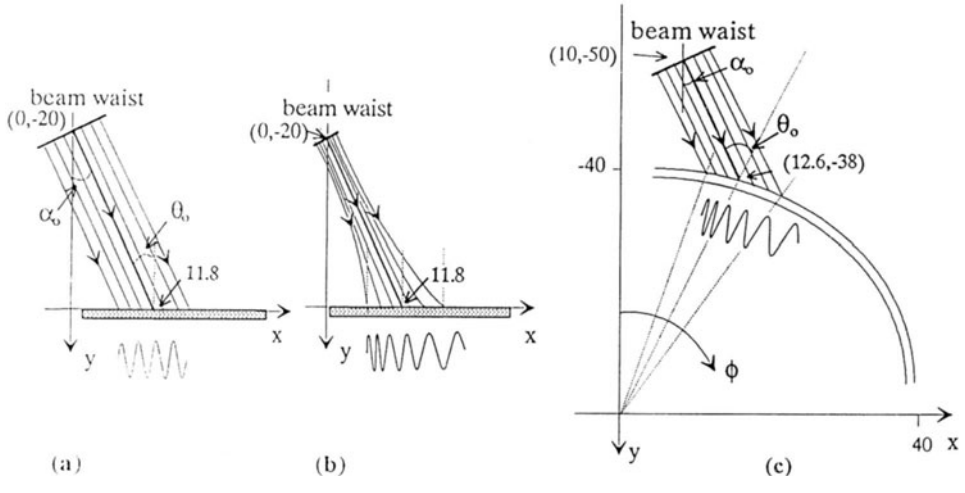

Fig.1 Schematization of interaction regions created on plane and cylindrical interfaces by various incident beams. The equiamplitude contours (phase paths) of the beams are shown up to the (1/e) contours that define the effective beam widths. Wavenumber periodicities induced by phase matching (wavevector projection onto the interface) are shown below the interface. θ_o=beam axis incidence angle. a) Well-collimated wide-waisted beam; plane interface. Periodicity along interface nearly constant (parallel phase paths, uniform projections). b) Diverging narrow-waisted beam; planar interface. Periodicities along interface vary from rapid to slow (diverging phase paths, nununiform projections). c) Well-collimated beam as in a); cylindrical interface. Curvature induces periodicities along interface analogous to those in (b) (parallel phase paths, nonuniform projections). All distances are normalized to wavelength in fluid $\lambda_f=2\pi/k_f$.

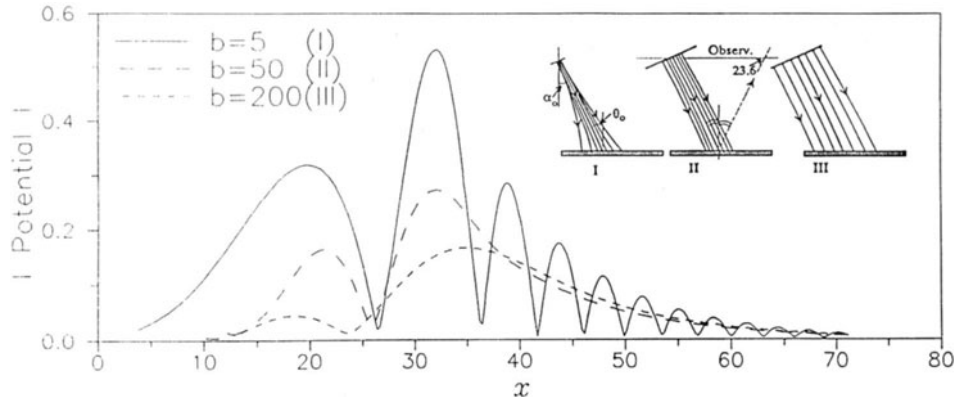

Fig.2 Detailed comparisons of total potential field magnitudes away from a plane water-aluminum interface, generated by various beams incident at the leaky Rayleigh wave angle $\theta_p=30.593^o$. Beam waists located at $(x',y')=(0,-20)$ (coordinate designations as in Fig.1). Beam Fresnel lengths: $b=5$, 50, and 200. Corresponding 1/e widths at the waists: $w_o=1.3$, 4, and 8. Beam launching angle with respect to y axis: $\alpha_o=30.593^o$. Observer at $y=-20$, in the plane passing through the incident beam waist. Schematics in insets show incident beam parameters, (1/e) beam contours and phase paths: strongly divergent, "narrow" well collimated, wide well collimated. The geometrically reflected beam axis is drawn dashed. Plots show total potential magnitudes computed from (6), established by interference between reflected and leaky wave fields (incident field does not reach region of observation). For interpretation, see Figs.1(a) and 1(b), and discussion in the text.

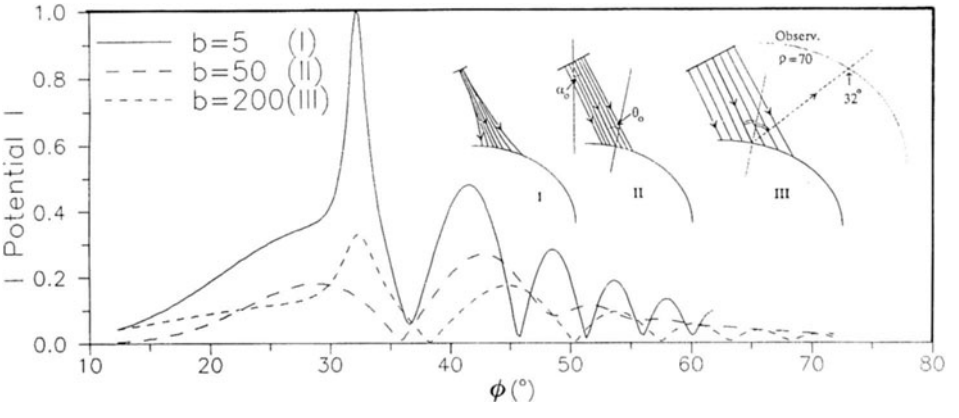

Fig.3 As in Fig.2, but for cylindrical interface, with radius $a=40$. Beam waists located at $(x',y')=(10,-50)$. Beam launching angle with respect to y axis: $\alpha_o=12.22^o$, corresponding to incidence angle $\theta_o=30.593^o$ on cylindrical interface. Observer located on circle $\rho=70$. Plots show total potential magnitudes computed from (7). For interpretation, see Figs.1(b) and 1(c), and discussion in the text.

CONCLUSIONS

The CSP method has been shown to furnish a versatile algorithm for predicting interaction of arbitrarily collimated quasi-Gaussian beams with plane and cylindrical fluid-solid interfaces, at arbitrary incidence angles that include phase matching to leaky waves. The algorithm can be implemented numerically without difficulty, can be generalized to arbitrarily curved and layered configurations, and can be extended to three dimensions. Details pertaining to the present applications and extensions will be submitted elsewhere for publication.

ACKNOWLEDGEMENT

This work has been supported by the U.S. Air Force Office of Scientific Research under Grant No. AFOSR-86-0318 and also, during its last phase, by the David Taylor Research Center under subcontract from Johns Hopkins University.

REFERENCES

1 H. L. Bertoni and T. Tamir, Appl. Phys.Vol.2, 157-172 (1973).
2 T. J. Plona, L. E. Pitts, and W. G. Mayer, J. Acoust. Soc. Am., Vol.59, 1324-1328 (1976).
3 L. E. Pitts, T. J. Plona, and W. G. Mayer, J. Acoust. Soc. Am., Vol.60, 374-377 (1976).
4 L. E. Pitts, T. J. Plona, and W. G. Mayer, IEEE Trans. Sonics Ultrason Vol.24, 101-109 (1977).
5 T. D. K. Ngoc and W. G. Mayer, J. Acoust. Soc. Am., Vol.67, 1149-1152 (1980).
6 J. M. Claeys and O. Leroy, J. Acoust. Soc. Am., Vol.72, 585-590 (1982).
7 J. Pott and J. G. Harris, J. Acoust. Soc. Am., Vol.76, 1829-1838 (1984).
8 H. Schmidt and F. B. Jensen, J. Acoust. Soc. Am., Vol.77, 813-825 (1985).
9 M. Rousseau and Ph. Gatignol, J. Acoust. Soc. Am., Vol.78, 1859-1867 (1985).
10 M. Rousseau and Ph. Gatignol, J. Acoust. Soc. Am., Vol.80, 325-332 (1986).
11 H-C. Choi and J. G. Harris, Wave Motion, Vol.11, 383-406 (1989).
12 L. B. Felsen, Geophy. J. R. Astron. Soc. Vol.79, 77-88 (1984).
13 M. Couture and P. A. Belanger, Phys. Rev. A Vol.24, 355-359 (1981).
14 L. B. Felsen and N. Marcuvitz, Radiation and Scattering of Waves (Prentice Hall, Englewood Cliffs, N.J., 1973).
15 L. B. Felsen, J. M. Ho, and I. T. Lu, J. Acoust. Soc. Am., Vol.87, 543-569 (1990).
16 Detailed manuscript to be submitted to J. Acoust. Soc. Am.